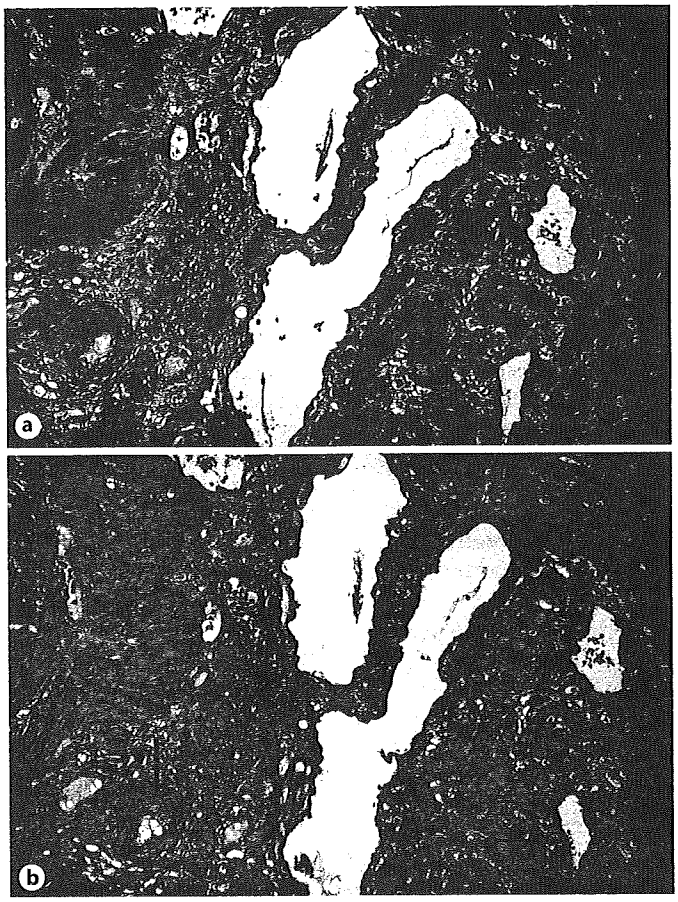

Fig. 1. Case 1: 30 min postpartum. Endometrial side. On the endometrial side, the IEL around the arteries was disrupted (arrow: artery). **a** HE. **b** Elasitca-van Gieson. ×10.

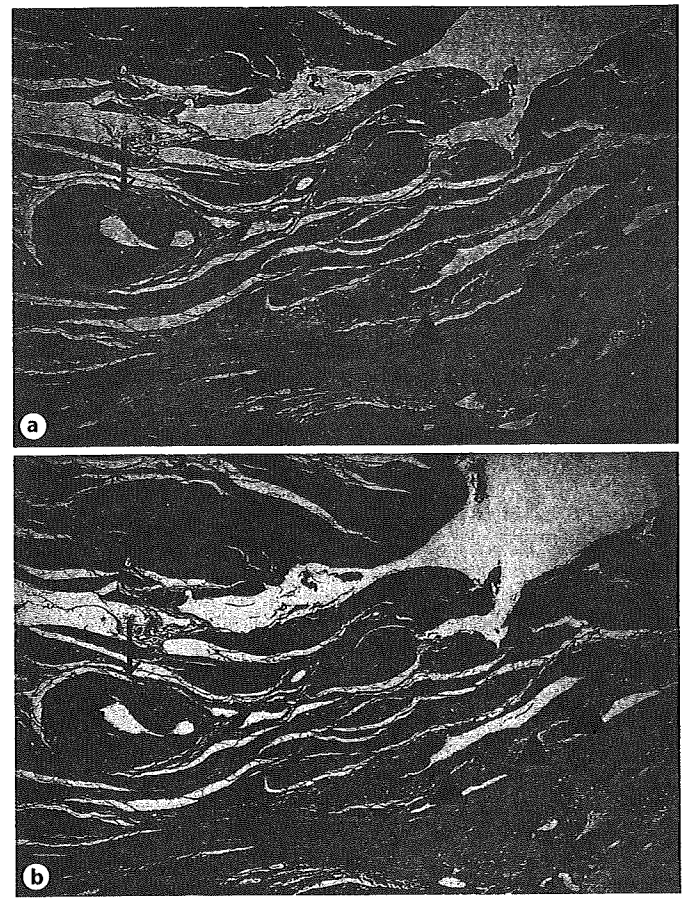

Fig. 2. Case 1: serosal side. Single layer of IEL and slightly thickened intima (arrow: artery, arrowhead: vein). **a** HE. **b** Elastica-van Gieson. ×10.

In this study, we examined the morphological process of uterine vascular involution and the expression of the oxytocin receptor (OTR) in uteri removed due to severe cervical laceration or uterine rupture.

Materials and Methods

Among 80 cases of hysterectomy due to postpartum hemorrhage at Osaka City University Hospital and Osaka Medical Center and Research Institute for Maternal and Child Health between January 1982 and December 2003, 15 cases (18.75%) of severe cervical laceration or uterine rupture were diagnosed based on clinical findings and gross inspection. Each resected uterus was fixed in 10% neutralized buffered formalin immediately after hysterectomy, then serially sliced horizontally into 5- to 10-mm-thick slices, and inspected to identify the point of bleeding. The myometrium was cut into slices, embedded in paraffin and preserved at room temperature until use in this study. We excluded cases showing subinvolution of the uterus, placenta accreta, placenta increta, or abruption of the placenta, and cases suffering from disseminated intravascular coagulation or infection as indicated by laboratory data.

The slides were prepared as 4-μm sections and stained with hematoxylin-eosin and elastica-van Gieson (EVG). Immunohistochemical stainings were performed according to a previously described method [9–11]. We used antibodies as follows: anti-CD34 (NU-4A1, 1:50 dilution, Nichirei, Tokyo, Japan), anti-α-smooth muscle actin (1A4, 1:50 dilution, Dako Cytomation, Glostrup, Denmark), and antioxytocin receptor (2F8, 1:50 dilution, Rohto, Osaka, Japan). Immunoreactivities of these antibodies were detected with the Envision system (Dako Cytomation) according to the instruction manual. We further performed Victoria Blue staining to detect elastic fibers with immunohistochemical stainings. We examined 5–10 slides for each uterus. Some cases underwent immunohistochemical staining for cytokeratin (AE1+AE3, 1:150 dilution, Dako Cytomation) to rule out placenta accreta.

Table 2. Histological findings

No.	Time after delivery	Arteries on the endometrial side				Veins on the endometrial side	
		formation of IEL	amount of reconstructed IEL[1]	intimal thickening[2]	pattern of intimal thickening	IEL	intimal thickening[2]
1	0 h 15 min	hardly detected	–	–	–	not detected	–
2	0 h 30 min	hardly detected	–	–	–	not detected	–
3	5 h	thin and disruptive	++	+++	eccentric	not detected	–
4	5 h	hardly detected	+	+++	eccentric	not detected	–
5	5 h 5 min	double layer	+++	+++	eccentric	not detected	–
6	5 h 16 min	double layer	+++	+++	eccentric	not detected	–
7	5 h 40 min	double layer	+++	+++	eccentric	not detected	–
8	6 h 22 min	double layer	+	+++	eccentric	not detected	–
9	6 h 27 min	double layer	+++	+++	eccentric	not detected	–
10	6 h 48 min	double layer	+++	+++	eccentric	not detected	–
11	8 h	double layer	+++	+++	eccentric	not detected	–
12	9 h 40 min	single layer	+++	+++	eccentric	not detected	–
13	16 h	single layer	+++	+++	eccentric	not detected	–
14	110 h	single layer	+++	+++	eccentric	not detected	–
15	19 days	single layer	+++	–	–	thin	–
16	60 days	single layer	+++	–	–	thin	–
17	7 years	single layer	+++	–	–	thin	–
18	5 years	single layer	+++	–	–	thin	–
19	–	single layer	+++	–	–	thin	–
20	–	single layer	+++	–	–	thin	–
21	–	single layer	+++	–	–	thin	–
22	–	single layer	+++	–	–	thin	–

[1] Fragments of IEL/Full circumference of lumen: – = <25%; + = 25–50%; ++ = 50–75%; +++ = >75%.
[2] Intimal thickening: – = Same as null gravida; + = <1/3 of thickness of media; ++ = <2/3 of thickness of media; +++ = thicker than media.

In order to compare uterine vessel morphology and immunoreactivity in these early-postpartum patients, we selected 7 age-matched uterine samples obtained from patients who underwent hysterectomy due to cervical intraepithelial neoplasia (1 case at 60 days postpartum, 1 at 5 years postpartum, 1 at 9 years postpartum and 4 null gravida patients).

Changes in the uterine vessels were analyzed as described in cardiovascular pathology, i.e. thickening of the intima and appearance of the IEL [12].

Results

The interval between delivery and hysterectomy ranged from 15 min to 19 days (tables 1–3). All patients were multigravidae. Six cases were delivered by cesarean section. The patients with cervical laceration (cases 3–6, 8, 11, 13) had delivered at other hospitals and were transferred to our hospital due to massive bleeding and hypovolemic shock. They underwent suturing of cervical lacerations. All patients were administered uterotonic agents (oxytocin, prostaglandin $F_{2\alpha}$, ergometrin) and transfused. Thirteen of 15 cases underwent hysterectomy within 24 h; all of them were severely anemic and in pre-hypovolemic shock state.

We studied the elastic lamina by EVG or Victoria Blue staining. Immunohistochemically, we used CD34 to detect vascular lumens and anti-α-smooth muscle actin to identify the intima and media.

We noticed that the vascular involution process varied substantially between the serosal side (arcuate arteries and veins) and the endometrial side (radial arteries and veins). On the endometrial side, the IEL of arteries was disrupted in cases in which hysterectomy had been performed shortly after delivery (case 1, 2). Reconstruction of IEL and intima thickening were also undetectable (fig. 1a, b). On the other hand, on the serosal side,

Arteries on the serosal side		Veins on the serosal side	
formation of IEL	intimal thickening[2]	elastic fibers in media	intimal thickening[2]
single layer	+	–	–
single layer	+	–	–
single layer	+	–	–
single layer	+	–	–
single layer	+	–	–
single layer	+	–	–
single layer	+	–	–
single layer	+	–	–
single layer	+	–	–
single layer	+	–	–
single layer	+	–	–
single layer	+	–	–
single layer	+	–	–
single layer	+	+	–
single layer	–	+	–
single layer	–	radial scar	–
single layer	–	radial scar	–
single layer	–	radial scar	–
single layer	–	–	–
single layer	–	–	–
single layer	–	–	–
single layer	–	–	–

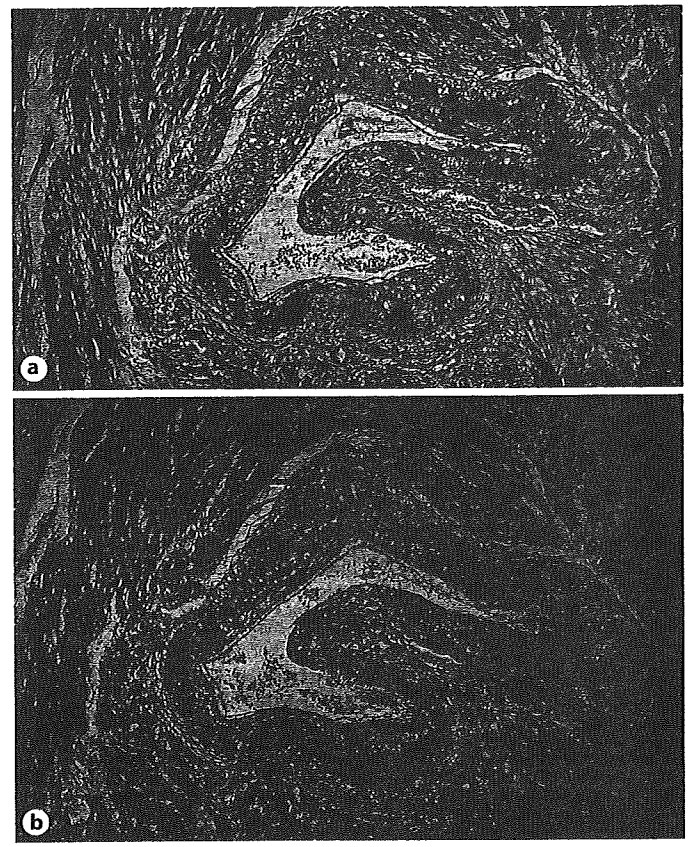

Fig. 3. Case 5: endometrial side. Double layers of IEL around arteries (asterisk). The intima was thickened and eccentric (arrow). **a** HE. **b** Elastica-van Gieson. ×10.

all arteries were surrounded by a single layer of IEL and had a slightly thickened intima (fig. 2a, b). After 5 h or more, we observed reconstruction and formation of IEL around arteries (fig. 3a, b). After 5 h, most arteries on the endometrial side were surrounded by double layers of IEL and thickened and eccentric intimas. The IEL was single-layered shortly after parturition (after 9 h, case 12), but intimal thickening disappeared (case 15) a long time after parturition. During this period, the arteries on the serosal side of the myometrium showed minimal changes in the IEL although intimal thickening was observed from very early to 5 h postpartum (fig. 4).

On the endometrial side, veins were dilated and medial smooth muscles could not be distinguished from those of the myometrium. Five hours after delivery, adventitiae were observed as an edematous space around veins. Elastic fibers in venous medias were scarce in the postpartum period. Thickening of the venous intimas was never observed (fig. 5a).

On the serosal side, we readily detected the venous medias shortly after delivery. The lumens had collapsed and the IEL was detected faintly around the veins. Intimal thickening was never detected. In cases 14 and 15, thin elastic fibers were detectable in the venous medias (fig. 5b). In the multigravida uteri, the caliber shrank, and the venous medias became very thick and displayed prominent elastic fibers (fig. 6). Similar findings were made in the uteri which had undergone parturition long before (cases 17 and 18).

In cases of very early postpartum (cases 1 and 2), OTR immunoreactivities were observed in the myometrium but not in vascular smooth muscles (fig. 7). Five hours after delivery, the receptor immunoreactivity became positive not only in the myometrium but also in the medial smooth muscles in arteries and veins (fig. 8). This

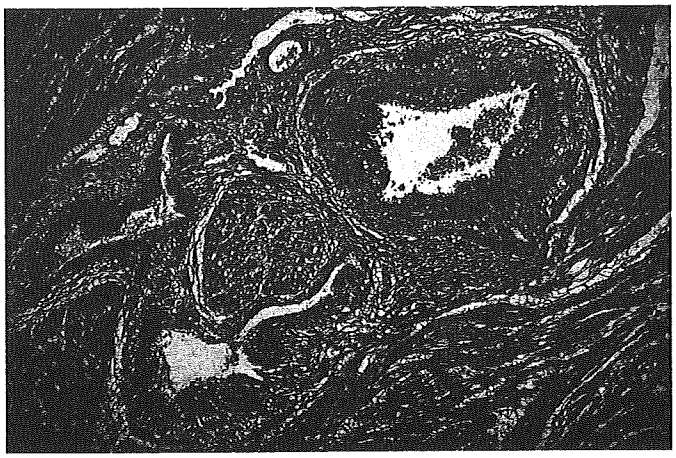

Fig. 4. Case 12: serosal side. Slight intimal thickening in arteries (arrow). Elastica-van Gieson. ×10.

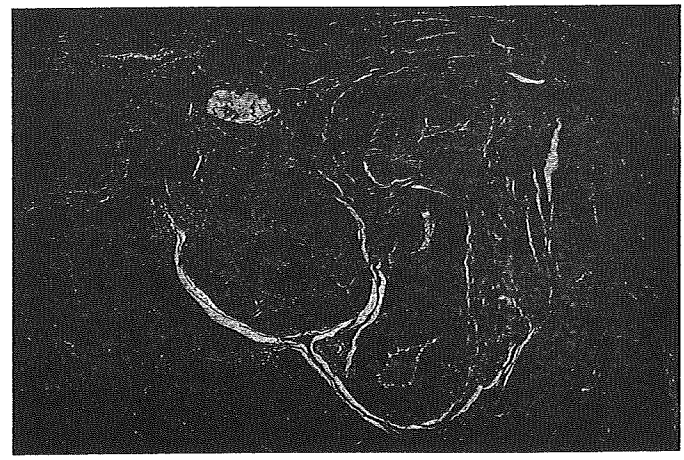

Fig. 6. Case 16: 60 days postpartum, radial elastic fibers are visible. Elastica van Gieson. ×4.

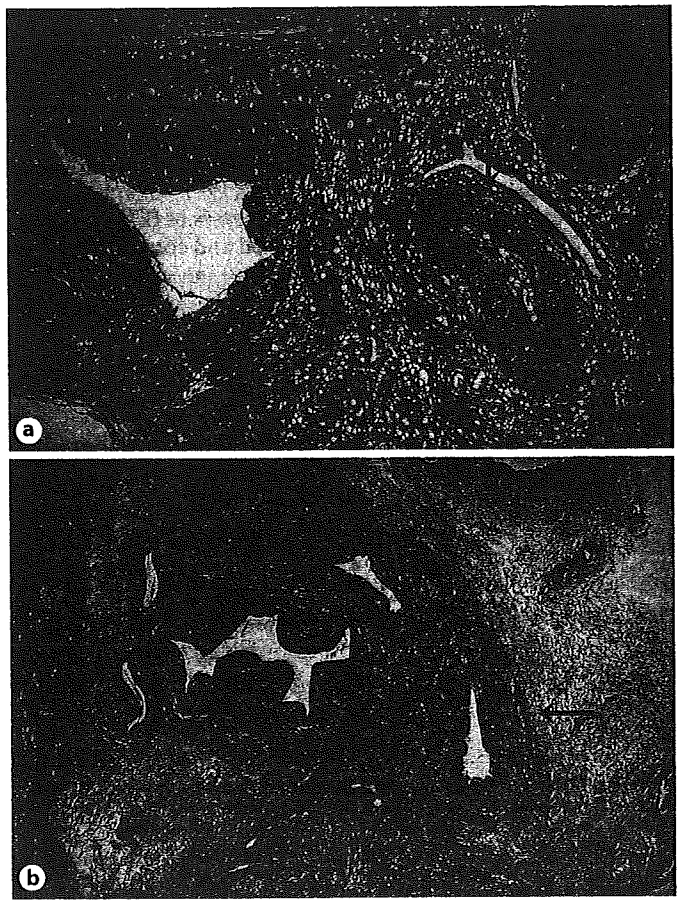

Fig. 5. Case 15. **a** Endometrial side. Elastic fibers were scarce in the vein media (asterisk). A double-layered IEL was detected in the artery (arrow). **b** Serosal side. Elastic fibers were detected in the media (arrow). **a**, **b** Elastica-van Gieson. ×10.

Table 3. Expression of OTR

No.	Time after delivery	Labor	Myometrium	Artery media	Vein media
1	0 h 15 min	+, induced	++	–	–
2	0 h 30 min	+, induced	ND	ND	ND
3	5 h	+, spontaneous	+	–	–
4	5 h	+, spontaneous	+	–	+
5	5 h 5 min	+, spontaneous	+	+	+
6	5 h 16 min	+, spontaneous	+	–	–
7	5 h 40 min	+, spontaneous	+	–	–
8	6 h 22 min	+, spontaneous	+	+	+
9	6 h 27 min	+, induced	+	+	+
10	6 h 48 min	–	+	–	+
11	8 h	+, spontaneous	+	+	+
12	9 h 40 min	–	+	+	+
13	16 h	+, spontaneous	+	+	+
14	110 h	–	+	+	+
15	19 days	+, spontaneous	+	–	–
16	60 days		–	–	–
17	7 years		–	–	–
18	5 years		–	–	–
19	–		–	–	–
20	–		–	–	–
21	–		–	–	–
22	–		–	–	–

ND = Not done; – = negative; + = positive.

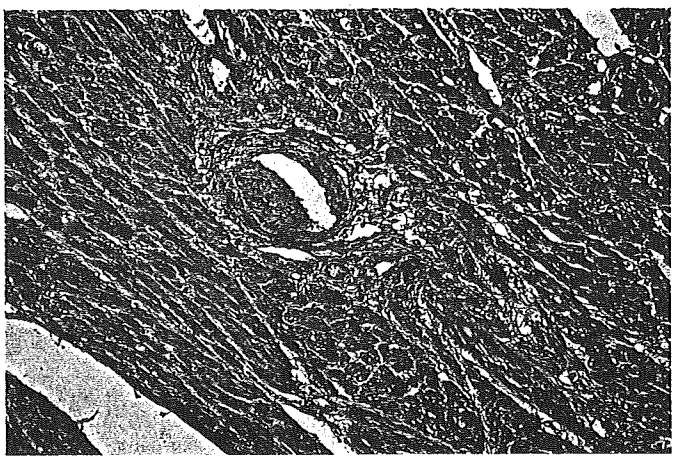

Fig. 7. Case 1: only the myometrium was positive for the OTR. The medias of arteries were negative for the OTR. OTR plus Victoria Blue. ×40.

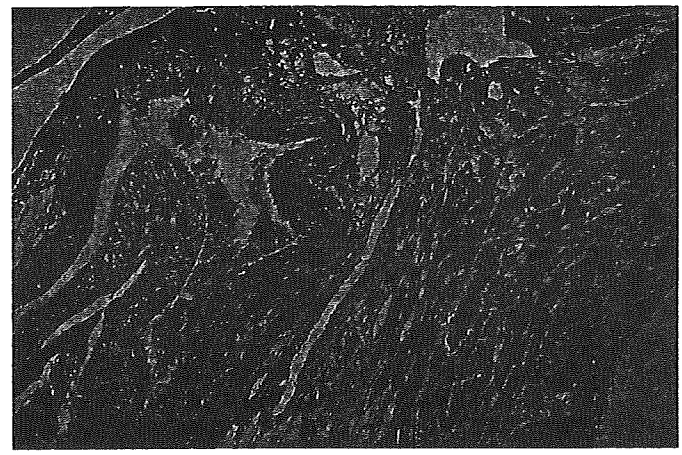

Fig. 8. Case 5: both the myometrium and vascular wall smooth muscles were positive for the OTR. OTR plus Victoria Blue. ×40.

change was observed both on the endometrial and serosal sides; the immunoreactivity disappeared within a few days postpartum (table 3).

There was 1 preterm case (case 14), but we could not detect any morphological or immunohistochemical differences between the samples obtained from preterm and term patients.

Discussion

Several reports about changes in uteroplacental arteries during the involution process have been published using the uteri or curettage specimens from late-postpartum patients [3, 5, 13]. In 1968, Anderson and Davis [4] focused on the vascular changes of the placental site during involution. However, they did not examine vascular remodeling using materials up to 24 h after delivery.

In this report, we precisely analyzed 13 uteri obtained following hysterectomy performed within 24 h postpartum and samples obtained during the puerperium. In a previous report, intimal thickening and hyalinization of the arterial medias on the endometrial side were noted at 1 and 3 days postpartum [4]. Intimal thickening was already observed 5 h postpartum. Moreover, we found that there were double layers of IEL 5 h postpartum. Anderson et al. [4] showed morphological differences between the endometrial and serosal sides of the uterus 1–3 days after delivery. We found that these differences occurred earlier, i.e. 5 h after delivery. In addition, we found that prominent elastic fibers in the walls of veins located on the serosal side were characteristic of multigravidae and persisted for a long time. These findings are similar to phlebosclerosis of esophageal varices [14]. Drastic increases in blood flow during pregnancy markedly dilate arteries and veins and then, after parturition, blood flow decreases very rapidly. This marked change in blood flow causes venous sclerosis.

Oxytocin plays important roles in uterine involution by inducing tonic and phasic contractions. In the very early period after parturition (cases 1, 2) OTR was localized only in the smooth muscle of the myometrium, but was negative in the smooth muscles of arterial medias. This pattern is similar to findings in our previous report [9]. However, we noticed that OTR immunoreactivity also appeared in the medias of arteries and veins. We could not determine whether this OTR is functional, but it seems physiologically reasonable to compress vessels using oxytocin to reduce uterine blood flow during the early puerperium period.

The series of patients examined here received many kinds of medication to treat hemorrhage or hypovolemic shock. These treatments may have had some effect on uterine vessels. Among them, ergonovine results in nonphysiological tonic uterine contraction without relaxation. Ergonovine sometimes induces systemic vasoconstriction and severe hypertension [15]. These medications may affect blood vessels and cause more rapid and marked vascular changes as observed here. Further experiments

are required to analyze the effects of medications on vessels using model animals.

In conclusion, uterine vessel remodeling occurs shortly after delivery. Elucidation of the mechanism of this rapid remodeling will help to understand the mechanism of the involution process and the management of postpartum hemorrhage.

Acknowledgement

This study was supported by Grants-in-Aid for Scientific Research from the Ministry of Education, Culture, Sports, Science, and Technology of Japan.

References

1 Robertson WB, Manning PJ: Elastic tissue in uterine blood vessels. J Pathol 1974;112:237–243.
2 Robertson WB, Brosens I, Dixon G: Uteroplacental vascular pathology. Eur J Obstet Gynec Reprod Biol 1975;5:47–65.
3 Paalma RJ, Mich GR, McElin TW: Noninvolution of the placental site. Am J Obstet Gynecol 1959;78:898–907.
4 Anderson WR, Davis J: Placental site involution. Am J Obstet Gynecol 1968;102:23–33.
5 Andrew AC, Bulmer JN, Wells M, Morrison L, Buckley CH: Subinvolution of the uteroplacental arteries in the human placental bed. Histopathology 1989;15:395–405.
6 Vedernikov YP, Betancourt A, Wentz MJ, Saade GR, Garfield RE: Adaptation to pregnancy leads to attenuated rat uterine artery smooth muscle sensitivity to oxytocin. Am J Obstet Gynecol 2006;194:252–260.
7 Evans JJ: Oxytocin in the human-regulation of derivations and destinations. Eur J Endocrinol 1997;137:559–571.
8 Chua S, Arulkumaran S, Lim I, Selamat N, Ratnam SS: Influence of breast feeding and nipple stimulation on postpartum uterine activity. Br J Obstet Gynaecol 1994;101:804–805.
9 Kimura T, Takemura M, Nomura S, Nobunaga T, Kubota Y, Inoue T, Hashimoto K, Kumazawa I, Ito Y, Ohashi K, Koyama M, Azuma C, Kitamura Y, Saji F: Expression of oxytocin receptor in human pregnant myometrium. Endocrinology 1996;137:780–785.
10 Kimura T, Ito Y, Einspanier A, Tohya K, Nobunaga T, Tokugawa Y, Takemura M, Kubota Y, Ivell R, Matsuura N, Saji F, Murata Y: Expression and immunolocalization of the oxytocin receptor in human lactating and non-lactating mammary glands. Human Reprod 1998;13:2645–2653.
11 Ito Y, Kobayashi T, Kimura T, Matuura N, Wakasugi E, Takeda T, Shimano T, Kubota Y, Nobunaga T, Makino Y, Azuma C, Saji F, Monden M: Investigation of the oxytocin receptor expression in human breast cancer tissue using newly established monoclonal antibodies. Endocrinology 1996;137:773–779.
12 Rosai J: Rosai and Ackerman's Surgical Pathology, ed 9. Philadelphia, Mosby, 2004.
13 Gainey HL, Nicolay KS, Lapi A: Noninvolution of the placental site: clinical and pathological studies. Am J Obstet Gynecol 1955; 69:558–572.
14 Davies JD: The oesophagus and stomach; in Whitehead R (ed): Gastrointestinal and Oesophageal Pathology. Edinburgh, Churchill Livingstone, 1989, pp 543–559.
15 Cunningham FG: Normal labor and delivery; management of the third stage of labor; in Cunningham FG et al (eds): Williams Obstetrics, ed 22. New York, McGraw-Hill 2005, pp 431–434.

PEDIATRICS INTERNATIONAL VOLUME 51 NUMBER 6 DECEMBER 2009

Official Journal of the Japan Pediatric Society

Congenital systemic juvenile xanthogranuloma with placental lesion

Makoto Takeuchi, Masahiro Nakayama, Akiko Nakano, Hiroyuki Kitajima and Akihisa Sawada

Submit your article online at
http://mc.manuscriptcentral.com/ped

ISSN 1328-8067

WILEY-BLACKWELL

www.blackwellpublishing.com/ped

Pediatrics International

EDITOR-IN-CHIEF
Norikazu Shimizu, Tokyo

ASSOCIATE EDITOR
Yoichi Sakakihara, Tokyo

ASSISTANT EDITORS

Katsuhiro Arai, Tokyo
Midori Awazu, Tokyo
Ikuko Hara, Tokyo
Kazushige Ikeda, Tokyo
Masami Inoue, Osaka
Ayano Inui, Tokyo
Yasuhiko Itoh, Tokyo
Masaya Kubota, Tokyo
Masaru Miura, Tokyo
Hiroshi Mochizuki, Tokyo
Yoshiyuki Ohtomo, Tokyo
Shinji Saito, Hokkaido
Isao Shiraishi, Osaka
Junko Takita, Tokyo
Shoji Tsuji, Osaka
Tatsuhiko Urakami, Tokyo
Yoshiyuki Yamada, Gunma

EDITORIAL BOARD

Kiyoshi Hayasaka, Yamagata
Hirokazu Kanegane, Toyama
Susumu Kanzaki, Tottori
Atsushi Manabe, Tokyo
Yoichi Matsubara, Sendai
Hiroyuki Nunoi, Miyazaki
Kayoko Saito, Tokyo
Yoshihiro Takeuchi, Shiga
Hajime Togari, Nagoya
Hiroaki Tsutsumi, Hokkaido
Yukishige Yanagawa, Tokyo

ADVISORY BOARD

Hiroatsu Agata, Aichi
Yoshimitsu Fukushima, Nagano
Shigeharu Hosono, Tokyo
Kazumoto Iijima, Tokyo
Yuko Ishizaki, Osaka
Seigo Korematsu, Oita
Haruo Kuroki, Chiba
Satoshi Kusuda, Tokyo
Takashi Nakano, Mie
Kandai Nozu, Kobe
Yasuhiro Okamoto, Kagoshima
Torayuki Okuyama, Tokyo
Keiichi Ozono, Osaka
Tatsuro Tajiri, Fukuoka
Shori Takahashi, Tokyo
Masato Takase, Tokyo
Hidetaka Tanaka, Osaka
Hajime Togari, Nagoya
Hirokazu Tsukahara, Fukui
Susumu Yokoya, Tokyo

INTERNATIONAL ADVISORY BOARD

Herbert T Abelson, USA
John Court, Australia
Ihsan Dogramaci, Turkey
Robert J Haggerty, USA
Lars Å Hanson, Sweden
Zai-Fang Jiang,
People's Republic of China
Vladimir K Kozlov, Russia
Leonard M Linde, USA
Hung-Chi Lue, Taiwan
A Majid Molla, Kuwait
Perla Santos Ocampo, Philippines
Stephen J Oppenhemier, UK
Mitrohan J Studenikin, Russia
Prasong Tuchinda, Thailand
Rolf Zetterstrom, Sweden

EDITORIAL SECRETARY
Kumiko Asanuma, Tokyo

LANGUAGE CONSULTANTS
Geoffrey Barraclough, Kobe
Rousei Hamada, Tokyo

Aims and Scope: *Pediatrics International* is the official English language journal of the Japan Pediatric Society and publishes articles of scientific excellence in pediatrics and child health delivery. An official Japanese language journal is also published by the Society: the 'Journal of the Japan Pediatric Society'.
Pediatrics International encourages submissions from all authors throughout the world. Manuscripts are judged by two experts solely on the basis of their contribution of original data and ideas and their presentation. All manuscripts must comply with the Instructions for Authors.

Abstracting and Indexing Services: The Journal is indexed by Abstracts on Hygiene and Communicable Diseases, ASSIA, Biological Abstracts (BIOSIS), Biomedical Reference (EBSCO), CancerLIT, Chemical Abstracts, CINAHL, Current Contents/Clinical Medicine, Dairy Science Abstracts, EMBASE/Excerpta Medica, Helminthological Abstracts, Ingenta, InPharma Weekly, JOIS, Journals@Ovid, Kidney, MEDLINE, Nutrition Abstracts and Reviews, Nutrition Research Newsletter, Pharmacoeconomics and Outcomes News, ProQuest, Reactions Weekly, Research Alert, Science Citation Index, SciSearch, SCOPUS, Tropical Diseases Bulletin.

Address for Editorial Correspondence: Norikazu Shimizu MD, Editor-in-Chief, *Pediatrics International*, Japan Pediatric Society, 4F Daiichi Magami Bldg, 1-1-5 Koraku, Bunkyo-Ku, Tokyo 112-0004, Japan (tel: (+81) 3 3818 0091; fax: (+81) 3 3816 6036).

Disclaimer: he Publisher, Society and Editors cannot be held responsible for errors or any consequences arising from the use of information contained in this journal; the views and opinions expressed do not necessarily reflect those of the Publisher, Society and Editors, neither does the publication of advertisements constitute any endorsement by the Publisher Society and Editors of the products advertised.

Journal compilation © 2009 Japan Pediatric Society.

Cover image: ^{99m}Tc scintigraphy showing multiple osteomyelitis in chronic granulomatous disease before bone marrow transplantation. See pages 838-841.

For submission instructions, subscription and all other information visit www.blackwellpublishing.com/ped.

This journal is available online at Wiley InterScience. Visit **www.interscience.wiley.com** to search the articles and register for table of contents and e-mail alerts.

Access to this journal is available free online within institutions in the developing world through the HINARI initiative with the WHO. For information, visit www.healthinternetwork.org.

ISSN 1328-8067 (Print)
ISSN 1442-200X (Online)

PED.JEB.Dec09

delay in ossification and eventual hyperlaxity of these synchondroses may cause deformation of the skull base. As exemplified in the present case, a diagnosis of HCS is generally delayed because the dysmorphic features of the disorder are individually subtle, and acro-osteolysis does not develop at younger ages. As in the present case, recent imaging modalities, for example MRI, facilitate the diagnosis of platybasia. Thus, platybasia identified in infancy and in young children may be taken as an early diagnostic sign of HCS in an appropriate clinical setting. Platybasia is seen as a component of isolated anomalies of the craniovertebral junction and as a result of abnormal softening of the skull base in a few genetic disorders, such as osteogenesis imperfecta. The differential diagnosis between these conditions and HCS is straightforward on clinical and radiological grounds.

The early onset of hydrocephalus is the second feature that merits comment. Platybasia leads to basilar impression, and basilar impression can cause neurological symptoms and hydrocephalus. Basilar invagination in HCS is believed to be exacerbated as a result of osteoporosis that progresses with age. All HCS patients with hydrocephalus reported so far developed hydrocephalus in late childhood. In contrast, the present patient first exhibited hydrocephalus at 5 months of age, it not being evident at birth. Further experience is required to determine whether or not such rapid development of hydrocephalus is common in HCS.

The third was bent or serpentine fibulae, which are a principal feature of SFPKS. SFPKS is a recently recognized disorder characterized by an unusual facial appearance, short stature, polycystic kidneys, and S-shaped and elongated fibulae. SFPKS was first confused with Melnick–Needles syndrome (MNS; 309350), which has been proven to belong to a group of disorders caused by mutations of the *FLNA* gene.[3] SFPKS, however, does not exhibit a few hallmarks of MNS, such as twisted ribs, cortical irregularities of the long bones, and abnormal lateral constriction of the iliac bones. Later, the phenotypic similarities between SFPKS and HCS, including serpentine or bent fibulae, were noted. Ramos *et al.* reported that HCS and SFPKS represent a single entity with variable degrees of expression.[4] The present patient provided further support for this hypothesis. The pathogenesis of HCS syndrome remains unknown. Classical investigations focused on the acro-osteolysis and high-turnover osteoporosis in HCS, and led to a few hypotheses, such as a dysfunction of osteoblasts and/or osteoclasts, and an imbalance between bone formation and resorption caused by a local-acting substance that activates osteoclasts.[5–7] The similarity, however, of HCS, SFPKS, and MNS indicates the direction of future investigations. Filamin A, encoded by the *FLNA* gene (the disease-causing gene of MNS), is a component of the cytoskeleton and closely interacts with transforming growth factor-β signaling pathways. These disorders await further investigations on filamin-related signaling pathways.

References

1 Brennan AM, Pauli RM. Hajdu-Cheney syndrome: Evolution of phenotype and clinical problems. *Am. J. Med. Genet.* 2001; **100**: 292–310.
2 Faure A, David A, Moussally F *et al.* Hajdu-Cheney syndrome and syringomyelia. Case report. *J. Neurosurg.* 2002; **97**: 1441–6.
3 Albano LM, Bertola DR, Barba MF, Valente M, Robertson SP, Kim CA. Phenotypic overlap in Melnick-Needles, serpentine fibula-polycystic kidney and Hajdu-Cheney syndromes: A clinical and molecular study in three patients. *Clin. Dysmorphol.* 2007; **16**: 27–33.
4 Ramos FJ, Kaplan BS, Bellah RD, Zackai EH, Kaplan P. Further evidence that the Hajdu-Cheney syndrome and the "serpentine fibula-polycystic kidney syndrome" are a single entity. *Am. J. Med. Genet.* 1998; **78**: 474–81.
5 Iwaya T, Taniguchi K, Watanabe J, Iinuma K, Hamazaki Y, Yoshikawa S. Hajdu-Cheney syndrome. *Arch. Orthop. Trauma. Surg.* 1979; **95**: 293–302.
6 Elias AN, Pinals RS, Anderson HC, Gould LV, Streeten DH. Hereditary osteodysplasia with acro-osteolysis (the Hajdu-Cheney syndrome). *Am. J. Med.* 1978; **65**: 627–36.
7 Nunziata V, di Giovanni G, Ballanti P, Bonucci E. High turnover osteoporosis in acro-osteolysis (Hajdu-Cheney syndrome). *J. Endocrinol. Invest.* 1990; **13**: 251–5.

Congenital systemic juvenile xanthogranuloma with placental lesion

Makoto Takeuchi,[1,4] Masahiro Nakayama,[1] Akiko Nakano,[2] Hiroyuki Kitajima[2] and Akihisa Sawada[3]

Departments of [1]Pathology, [2]Neonatology and [3]Hematology/Oncology, Osaka Medical Center and Research Institute for Maternal and Child Health and [4]Department of Pathology, Ikeda Municipal Hospital, Osaka, Japan

Key words Langerhans cell histiocytosis, neonate, placenta, systemic juvenile xanthogranuloma.

Correspondence: Makoto Takeuchi, MD, Department of Pathology, Ikeda Municipal Hospital, 3-1-18 Jonan, Ikeda, Osaka 563-8510, Japan. E-mail; makoto-takeuchi@hosp.ikeda.osaka.jp

Received 19 September 2007; revised 28 December 2007; accepted 29 February 2008.
doi: 10.1111/j.1442-200X.2009.02932.x

Juvenile xanthogranuloma (JXG) is a cutaneous tumor of the histiocytic cell in infancy and early childhood, which is differentiated from Langerhans cell histiocytosis (LCH) and usually follows a benign course without treatment with gradual regression over approximately 3 years.[1] A few cases, however, have

© 2009 Japan Pediatric Society

demonstrated one or more extracutaneous viscera and rarely the disease has produced serious symptoms and has even been fatal.[2-4] We present a case of congenital systemic JXG with serious symptoms that was correctly diagnosed in the wake of a placental examination.

Case report

A 1907 g boy was born at 36 weeks gestation by emergency cesarean section due to intrauterine growth restriction and fetal distress. Apgar scores were 7 and 9 at 1 and 5 min, respectively. The infant demonstrated systemic petechiae and purpura with a subcutaneous solid nodule on the left femoral region (Fig. 1). Laboratory tests showed leukocytosis (18 300/μL), anemia (red blood cells 143×10^4/μL, hemoglobin 5.5 g/dL), thrombocytopenia (0.5×10^4/μL) and a slightly elevated level of C-reactive protein (1.5 mg/dL) suggestive of latent infection. The infant was transferred to Osaka Medical Center and Research Institute for Maternal and Child Health on the same day and full screening tests for infection were performed. Antibiotics and blood transfusions were initiated, but spike fever, tachypnea and hepatosplenomegaly developed and his clinical condition deteriorated further despite intensive therapy. All cultures were negative and there was no evidence of fetal infection. Bone marrow aspiration did not demonstrate any evidence of hemophagocytosis, but respiratory distress was progressively worsening. We started methylprednisolone therapy due to the deterioration. Symptoms improved although he needed a blood transfusion and steroid therapy. At that time, placental examination demonstrated some clusters of atypical small cells showing round to spindle shape in the villi, suggesting metastasis from an unknown origin (Fig. 2).

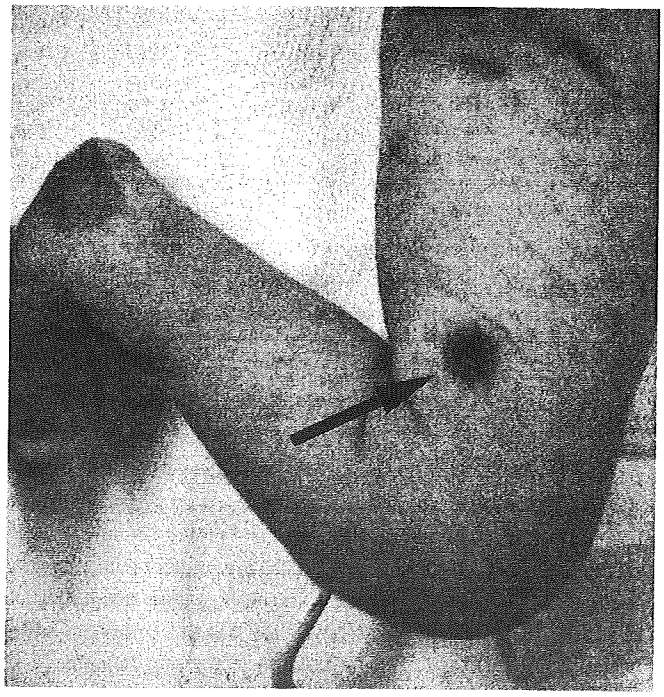

Fig. 1 Subcutaneous solid nodule in the left femoral region.

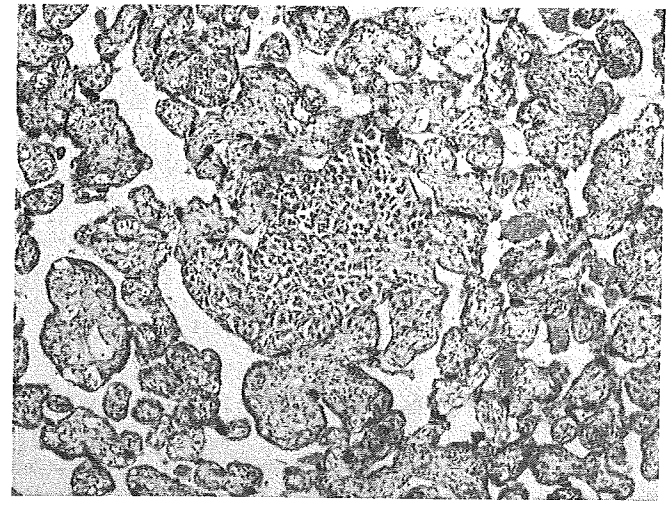

Fig. 2 Cluster of atypical small cells with a round–spindle shape in the villi.

We performed a skin biopsy of the subcutaneous solid nodule on his femoral region for diagnosis on the 18th day of life.

The lesion formed a well-circumscribed but non-encapsulated nodule that extended to the epidermal layer and into subcutaneous fat (Fig. 3a). These cells were mostly composed of mononuclear cells, which had round to elongate, bean-shaped nuclei with moderately dense, uniformly dispersed chromatin, variable conspicuous nucleoli and pale eosinophilic to finely vacuolated cytoplasm (Fig. 3b). There were few eosinophils. Occasionally, giant cells with peripherally or centrally aggregated nuclei were present, but Touton giant cells were not seen at all. These findings were suggestive of LCH but on immunhistochemistry the infiltrating histiocytic cells were positive for vimentin, CD68 and factor XIIIa, but negative for S100 protein and CD1a. We confirmed JXG. Additionally, the atypical cells of the placenta had positive staining for CD68 and factor XIIIa and negative staining for S100 protein and CD1a, which were correlated with JXG. Abdominal magnetic resonance imaging (MRI) demonstrated infiltration around the portal vein (Fig. 4). Finally, we diagnosed congenital systematic JXG based on the clinical features and pathologic findings of the skin and placenta. LCH-oriented chemotherapy was started on the 32nd day. He became free from blood transfusion 2 months after the initiation of the chemotherapy, and hepatosplenomegaly was resolved after 4 months. Follow-up MRI indicated marked resolution of the hepatic infiltration after 6 months. The 12 months of treatment were completed, and the infant has continued in complete remission for approximately 2 years.

Discussion

Histiocytosis syndromes are generally grouped into LCH and non-LCH. JXG is one of the most common disorders in the non-LCH group. The typical histologic appearance in JXG consists of a dense dermal infiltration of foamy histiocytes with Touton giant cells. JXG, however, represents a spectrum of the disease in which the dermal dendrocytes can have different levels

© 2009 Japan Pediatric Society

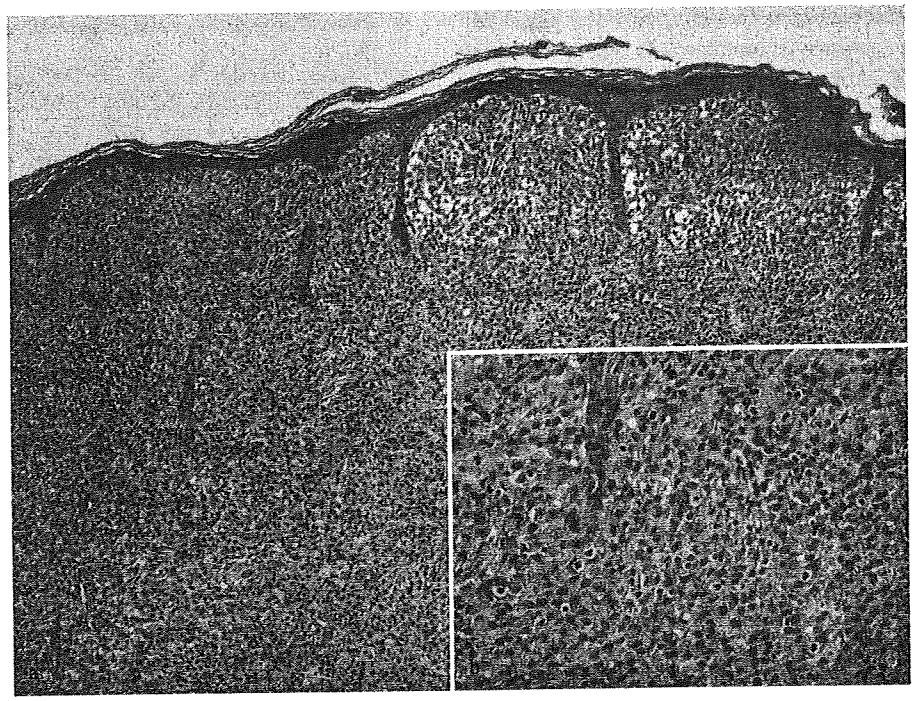

Fig. 3 (a) Low-magnification and (b) high-magnification (inset) views of infiltration of mononuclear cells without Touton cell in the subcutaneous solid nodule.

of maturation.[5] The early lesion consists of small–moderately sized mononuclear histiocytes with eosinophilic cytoplasm and displays a compact sheet-like infiltrate, which often has no or rare Touton giant cells. These findings are similar to those of LCH and obscure the diagnosis. At first, we assumed that the diagnosis would be LCH in the present case because of absent lipidization of histiocytes, intermixed eosinophils and the lack of Touton giant cells, but a differential diagnosis is easily possible on immunohistochemistry. Histiocytes in JXG show characteristics similar those of dermal dendrocytes, which are reactive with CD68 and Factor XIIIa and non-reactive to S100 protein and CD1a.

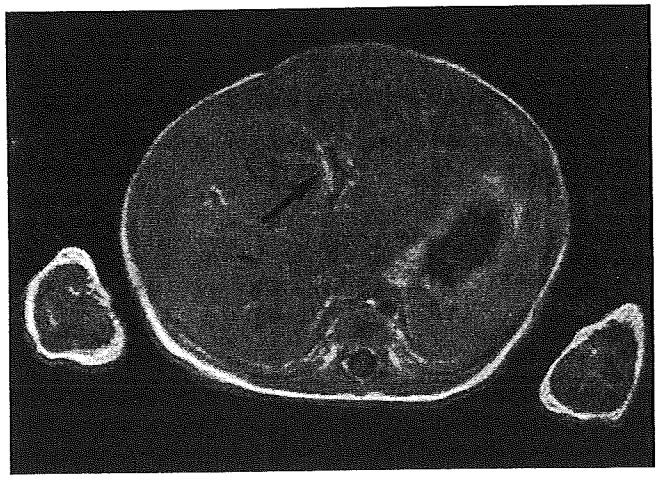

Fig. 4 Infiltration of juvenile xanthogranuloma cells around the portal vein on abdominal magnetic resonance imaging.

Systemic JXG is associated with one or more sites of extracutaneous involvement including liver, lung, spleen, kidney and central nervous system (CNS).[2–4] Almost all cases develop within 1 year or are present at birth. Some patients may develop serious symptoms and it may even become fatal. Recently, two large studies of JXG were performed.[2,3] Dehner reviewed eight children with systemic JXG among 174 cases.[2] Two of these patients died of hepatic failure at 1 month. Janssen and Harms reviewed five children with systemic JXG among 129 cases.[3] One patient died of multiple extensions of systemic JXG at 34 days. From the perspective of systemic JXG, Freyer *et al.* analyzed 36 cases from the literature as well as their own two patients.[4] Two patients died of progressive CNS lesions. Although the majority of systemic JXG regressed spontaneously, significant morbidity has been reported in a few cases, requiring systemic chemotherapy.[2–4,6] Several neonates had a presentation similar to that of the present patient, consisting of a skin lesion, hepatosplenomegaly and thrombocytopenia.[6–10] Some of these patients also had liver infiltration of JXG cells on either autopsy or liver biopsy. In the present case MRI showed infiltration around the portal vein, which we speculate is an indication of the same phenomenon as demonstrated in aforementioned cases.

The placental lesion in the present patient appears to be unique and may have contributed to the diagnosis. We initially suspected that this case involved severe neonatal infection because of the general condition, and started examinations including the placenta. We found some clusters of atypical cells in the villi after thorough examination of the placenta, and realized that a skin biopsy was necessary for diagnosis. Indeed, in systemic JXG, extracutaneous lesions are generally composed of

© 2009 Japan Pediatric Society

only mononuclear cells, mononuclear cells with an intermixture of spindle cells in the absence of multinuclear cells, or a nearly exclusive spindle cell proliferation with or without a collagenous background unlike the cutaneous lesions.[2] This was true of the placental lesion in the present case. In the literature there is no description of the placenta except in a case reported by Hu *et al.*, in which a placental lesion was not detected.[7] It is assumed that the placental lesion has not yet been noticed in congenital systemic JXG. It is therefore necessary to examine the placenta when we encounter congenital systemic JXG.

In conclusion, we should remember that some neonates with systemic JXG have severe symptoms and histopathology similar to LCH. Thus, we should perform further examinations including of the placenta to establish a correct diagnosis before therapy.

References

1 Weiss SW, Goldblum JR Benign fibrohistiocytic tumors. In: Weiss SW, Goldblum JR (eds). *Soft Tissue Tumor*, 4th edn. Mosby, St Louis, MO, 2001; 441–90.
2 Dehner LP. Juvenile xanthogranuloma in the first two decades of life: A clinicopathologic study of 174 cases with cutaneous and extracutaneous manifestations. *Am. J. Surg. Pathol.* 2003; **27**: 579–93.
3 Janssen D, Harms D. Juvenile xanthogranuloma in childhood and adulthood: A clinicopathologic study of 129 patients from the Kiel Pediatric Tumor Registry. *Am. J. Surg. Pathol.* 2005; **29**: 21–8.
4 Freyer DR, Kennedy R, Bostrom BC, Kohut G, Dehner LP. Juvenile xanthogranuloma: Forms of systemic disease and their clinical implication. *J. Pediatr.* 1996; **129**: 227–37.
5 Coffin CM. Fibrohistiocytic tumors. In: Coffin CM, Dehner LP, O'Shea PA (eds). *Pediatric Soft Tissue Tumor*. Williams & Wilkins, Baltimore, MD, 1997; 179–213.
6 Nakatani T, Morimoto A, Kato R *et al.* Successful treatment of congenital systemic juvenile xanthogranuloma with Langerhans cell histiocytosis-based chemotherapy. *J. Pediatr. Hematol. Oncol.* 2004; **26**: 371–4.
7 Hu WK, Gillian AC, Wiersma SR, Dahms BB. Fatal congenital juvenile xanthogranuloma with liver failure. *Pediatr. Dev. Pathol.* 2004; **7**: 71–6.
8 Kobayashi K, Imai T, Adachi S *et al.* Juvenile xanthogranuloma with hematologic changes in dizygotic twin: Report of two newborn infants. *Pediatr. Dermatol.* 1998; **15**: 203–6.
9 Favara B. Histopathology of the liver in histiocytosis syndromes. *Pediatr. Pathol. Lab. Med.* 1996; **16**: 413–33.
10 Eggli KD, Caro P, Quiogue T, Boal DKB. Juvenile xanthogranuloma: Non-X histiocytosis with systemic involvement. *Pediatr. Radiol.* 1992; **22**: 374–6.

Acute renal failure caused by fungus balls in renal pelvises

Kiyak Aysel,[1] Yilmaz Alev,[1] Canpolat Nur,[1] Aydogan Gonul,[2] Sander Serdar,[3] Korkmaz Orhan[4]

[1]Pediatric Nephrologist, Bakirkoy Maternity and Childrens Hospital, Pediatric Nephrology Department, [2]Chief of Department of Pediatrics, Bakirkoy Maternity and Childrens Hospital, Department of Pediatrics, [3]Pediatric Surgeon, Bakirkoy Maternity and Childrens Hospital, Pediatric Surgery Department, and [4]Radiologist, Bakirkoy Maternity and Childrens Hospital, Istanbul, Turkey

Key words *Candida albicans*, fungus ball.

Candida infection of the urinary tract is uncommon. It may occur as a part of systemic candidiasis or as a focal urinary tract infection in immunocompromised patients.[1,2] Candida infections are usually associated with one or more predisposing factors including prematurity, prolonged use of antibiotics or steroids, total parenteral nutrition, umbilical or bladder catheters, vesicoureteral reflux (VUR) and diabetes mellitus.[2–4]

Renal parenchyma, ureters or bladder may be affected by a fungal infection and the urinary tract can be obstructed by a fungus ball formation at any level.[1–3,5] Acute renal failure (ARF) caused by systemic candidiasis or obstruction of the urinary tract with fungus ball is a rare complication of fungal infections.[1,2,5–8] In the present report the case of a 3-month-old patient with ARF due to bilateral fungus ball in renal pelvis with ureteral extension is described.

Correspondence: Alev Yilmaz, MD, Pediatric Nephrology Department, Bakirkoy Maternity and Children's Hospital, Istanbul, Turkey. Email: alevyy@yahoo.com

Received 11 December 2007; accepted 18 March 2008.
doi: 10.1111/j.1442-200X.2009.02928.x

© 2009 Japan Pediatric Society

Case report

A 3-month-old male patient was admitted to Bakirkoy Maternity and Childrens Hospital with high fever. The family stated that the patient had been taken to another hospital with a complaint of cough 1 week previously and received i.m. ampicillin for pulmonary infection during 1 week before admission to Bakirkoy Maternity and Childrens Hospital.

From his past medical history we learned that he had been born at 2240 g in the 34th gestational week and intraventricular hemorrhage had been detected on cranial ultrasound. Thereafter post-hemorrhagic hydrocephaly had occurred and a ventriculoperitoneal shunt operation had been performed when he was 24 days old.

At admission his rectal temperature was 39.5°C. Blood pressure was within normal range for age. There were no lethargy, vomiting or diarrhea. His skin, eye, ear, fontanel, cardiac, pulmonary and abdominal examination were normal. We did not determine any signs of pulmonary infection on physical examination or chest radiogram. His white blood cell count

Pediatr Cardiol (2009) 30:343–346
DOI 10.1007/s00246-008-9308-y

CASE REPORT

Apical Hypertrophic Cardiomyopathy in Childhood: A Long-Term Follow-Up Report of Two Cases

Tomoyuki Miyamoto · Hitoshi Horigome · Satoru Kawano · Ryo Sumazaki

Received: 31 July 2008 / Accepted: 25 August 2008 / Published online: 4 October 2008
© Springer Science+Business Media, LLC 2008

Abstract We present two children with apical hypertrophic cardiomyopathy (APH), both of whom remained asymptomatic for more than 15 years. The inverted T-wave on electrocardiograms and myocardial hypertrophy mostly confined to the apical region on echocardiograms showed no significant changes during follow-up. Magnetic resonance imaging revealed a cavitylike portion at the apex in one case, but the diagnosis of noncompacted myocardium was unlikely because there was no blood communication with the true left ventricular cavity. The other case had typically thick and solid myocardium at the apex. The findings in these patients demonstrate that APH might present in childhood and suggest that the prognosis might be good.

Keywords Apical hypertrophic cardiomyopathy · Children · Noncompaction left ventricular myocardium · Giant negative T-wave

Introduction

Apical hypertrophic cardiomyopathy (APH) is a relatively rare variant of hypertrophic cardiomyopathy (HCM) and characterized by myocardial hypertrophy, predominantly in the left ventricular apical region, with spade-shaped left ventricular cavity and giant negative T-waves on the electrocardiogram (EKG) [1, 6, 8]. Prognosis of the disease is thought to be favorable, with a mortality rate lower than that of other types of HCM [5, 7]. Although there are many reports of patients with APH diagnosed in adult patients, especially in Asian countries [1], to our knowledge there are no reports of cases of APH diagnosed in childhood [3, 5, 7]. Sakamoto [5] reviewed 126 patients with APH, but no pediatric cases were included in that review. Here we report the clinical course of two cases with APH diagnosed at school age with follow-up for more than 15 years.

T. Miyamoto · H. Horigome (✉) · R. Sumazaki
Department of Child Health, Graduate School of Comprehensive Human Sciences, University of Tsukuba, Tsukuba 305-8575, Japan
e-mail: hhorigom@md.tsukuba.ac.jp

S. Kawano
Division of Cardiology, Department of Internal Medicine, Graduate School of Comprehensive Human Sciences, University of Tsukuba, Tsukuba 305-8575, Japan

Case Report

Case 1

A 6-year-old girl was referred to our hospital for further evaluation in view of an abnormal T-wave on an EKG incidentally noted on a routine health check program for entry to primary school. The patient had no family history of cardiac disease and had not experienced syncope, chest pain, or palpitation. Physical examination on referral was within normal limits. The EKG showed negative T-waves with slight ST depression in leads V4–6 (Fig. 1a). Echocardiography showed myocardial hypertrophy almost confined to the apical portion of the left ventricle (LV), resulting in a shallow apex, with increased LV dimension at the basal level to 43 mm with a shortening fraction of 35% (Fig. 2). These abnormalities warranted a follow-up cardiac catheterization. The LV pressure was 104/10 (systolic/end diastolic) mmHg without outflow tract pressure gradient, and the pulmonary arterial pressure was 34/14 mmHg. The LV end-diastolic volume index and

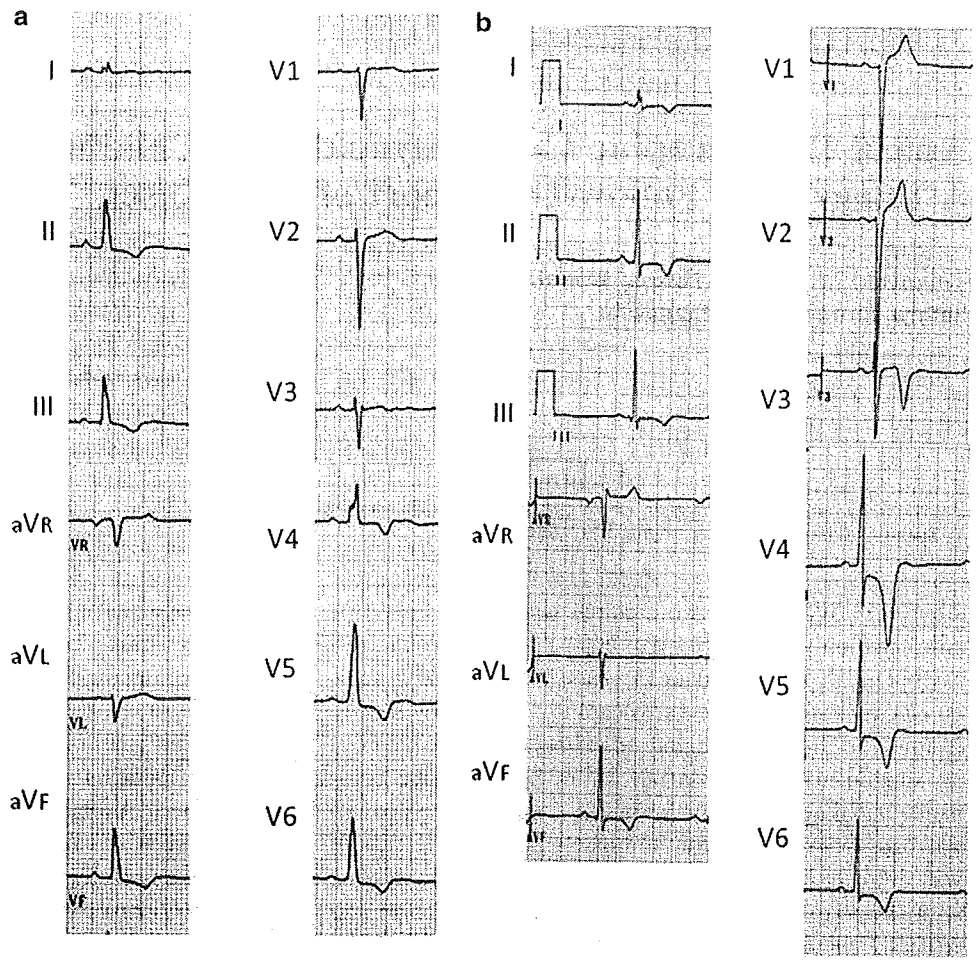

Fig. 1 Electrocardiogram of (**a**) Case 1 at age 6, showing negative T-waves in leads V4–6 and (**b**) Case 2 at age 13, showing giant negative T-waves in leads V3–5 with ST depression

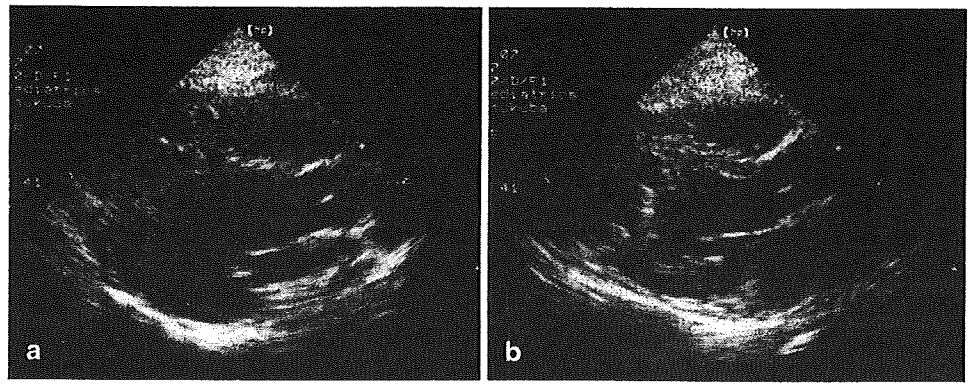

Fig. 2 Left ventricular long-axis view of echocardiograms of Case 1 in (**a**) end diastole and (**b**) end systole. Note the apical hypertrophy and resultant shallow bottom

ejection fraction were 98 ml/m^2 and 67%, respectively. Both myocardial scintigraphy using ^{201}Tl-Cl and ^{123}I-BMIPP showed low uptake at the apical area with the size of the area on ^{123}I-BMIPP being slightly larger than that on ^{201}Tl-Cl. During the next 15 years, the patient remained asymptomatic, the EKG showed no worsening, and echocardiography indicated no deterioration of LV function.

Case 2

A 13-year-old boy was referred to our hospital for evaluation of negative T-waves incidentally noted on an EKG for the first time on a routine health check program for entry to junior high school. The patient had no family history of cardiac disease and no complaints. Physical examination on presentation showed no

abnormalities, as in Case 1. The EKG showed giant negative T-waves with slight ST depression in the inferior and V3–5 leads (Fig. 1b). A diagnosis of APH was made based on echocardiographic findings. The end-diastolic LV dimension at the basal portion was increased to 55 mm and the shortening fraction (LVSF) was 40%. Cardiac catheterization showed normal LV pressure, volume, and ejection fraction (systolic/end-diastolic pressure = 89/5 mmHg, EDVI = 86 ml/m^2, EF 60%), and a typical spade-shaped configuration was noted on left ventriculography (Fig. 3). Both myocardial scintigraphy using ^{201}Tl-Cl and ^{123}I-BMIPP showed high uptake, in contrast to Case 1, in the apical area. However, the tracer uptake in the same apical region was slightly reduced on repeat ^{123}I-BMIPP study conducted at age 19. The patient remained asymptomatic and the T-wave on the annual EKG and LV function on echocardiography did not change significantly during the next 15 years.

Magnetic Resonance Imaging

Magnetic resonance imaging (MRI) was conducted in each case to evaluate the characteristics of apical myocardium. In Case 1, the MRI at age 20 showed a cavitylike area separate from the LV cavity (Fig. 4a). The density of this portion was halfway between free wall myocardium and true LV cavity. This apical portion had never been stained with contrast medium on left ventriculography and no color-Doppler signals entering the apical portion was observed, suggesting that this area did not communicate with the true LV cavity. It was possible that the myocardial tissue of this area was different from the normal myocardium and was suspected to be either ischemic fibrous tissue or noncompacted tissue, which could explain the low uptake on scintigraphy. On the other hand, the MRI of Case 2 taken at 28 years of age showed that the apical portion of the LV was composed of thickened homogeneous myocardium (Fig. 4b).

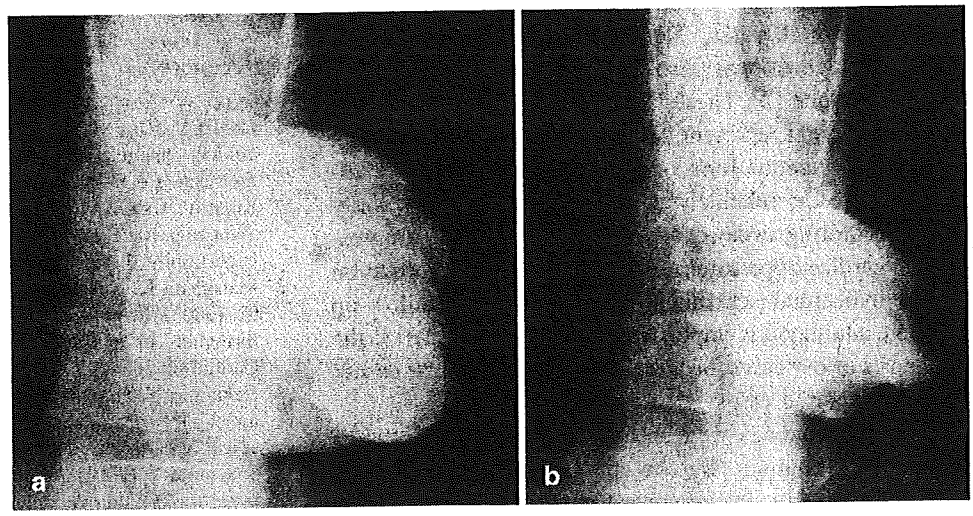

Fig. 3 Left ventricular angiograms of Case 2 in (**a**) end diastole and (**b**) end systole. Note the apical hypertrophy and typical spade-shaped LV cavity

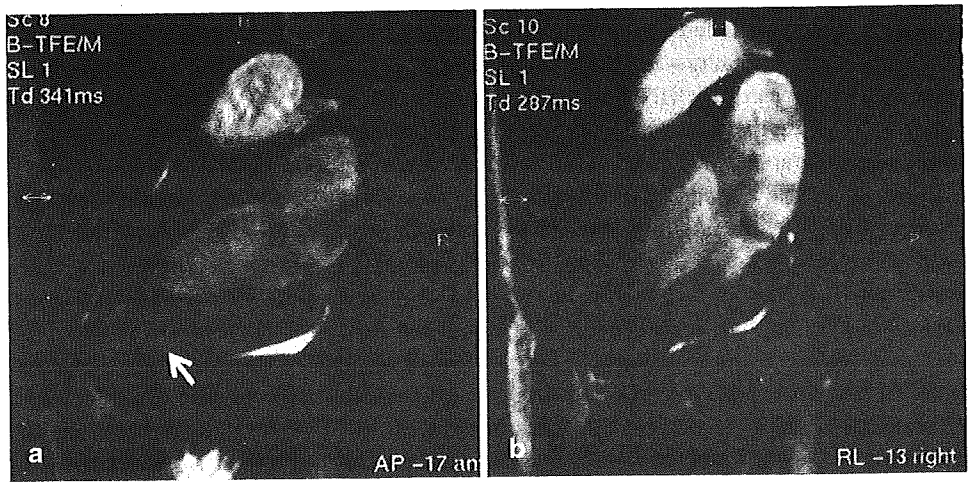

Fig. 4 MRI images of the left ventricle of (**a**) Case 1 and (**b**) Case 2. Note the cavitylike area (arrow) in Case 1, which is separate from true LV cavity. The density of this portion is halfway between free wall myocardium and true LV cavity. In Case 2, note the homogeneously hypertrophied myocardium in the apical region

Discussion

Apical hypertrophic cardiomyopathy is considered a rare variant of cardiomyopathy typically diagnosed in middle-aged individuals [1, 5]. To our knowledge, there are no pediatric cases reported in the literature [1, 5]. Both cases reported here were diagnosed incidentally during childhood at a routine health check conducted at school entry, based on abnormal EKG repolarization. Both patients remained asymptomatic during the follow-up period of more than 15 years. In this regard, we are unaware of any report that describes the long-term clinical course of APH over a period of >15 years from childhood to adulthood. It is notable that both patients remained asymptomatic and cardiac function did not deteriorate during the follow-up period.

In this report, the EKG findings remained almost unchanged in both cases. However, it has been reported that the characteristic giant negative T-wave disappears in some patients [2, 5]. Koga et al. [2] indicated that the giant negative T-wave disappeared in 31% of patients after a follow-up period of 5–9 years, and the frequency increased to 71% over 10 years. The disappearance of the giant negative T-waves was associated with a decrease in R-wave amplitude [2]. These EKG changes in some patients with APH might represent the progressive nature, although slow, of this unique form of cardiomyopathy [2]. In addition, despite the relatively good prognosis of APH, long-term monitoring occasionally exhibits a gradual progression of cardiac hypertrophy and apical aneurysm formation due to myocardial ischemia [3, 4]. Thus, a longer follow-up into late adulthood is important in order to characterize the prognosis of our cases, because age at diagnosis was earlier than the reported cases.

The MRI findings were intriguing. On both echocardiography and angiography, the apical portion of the LV in Case 1 appeared to be composed merely of hypertrophied myocardium. However, the MRI detected a cavitylike area separated by muscle from the real LV cavity (Fig. 4a).

With regard to differentiation of APH from another peculiar cardiomyopathy—idiopathic noncompaction left ventricular myocardium (INVM)—the latter could be excluded because there were no projecting muscles or deep recesses in the apical portion of the LV on both echocardiography and angiography. Matsubara et al. [3] investigated the effects of apical cavity obliteration by hypertrophied myocardium during systole in APH and found that severe obliteration induced myocardial ischemia, resulting in aneurysm formation. In Case 1, however, there was no blood inflow in the apical portion even at first presentation. Although scintigraphy indicated myocardial ischemia at the corresponding site, acquired isolation of the apical cavity was unlikely, making the diagnosis of INVM improbable. It is possible that the etiology of childhood APH is different from that of adulthood.

Conclusion

We report two cases of children with APH. Both cases remained asymptomatic during the follow-up period of more than 15 years, suggesting good prognosis of the disease; longer follow-up is needed to monitor for any complications. We recommend MRI examination to be part of APH assessment, as it can provide useful information about the nature of apical myocardial tissue.

References

1. Choi EY, Rim SJ, Ha JW et al (2008) Phenotypic spectrum and clinical characteristics of apical hypertrophic cardiomyopathy: multicenter echo-Doppler study. Cardiology 110:53–61
2. Koga Y, Katoh A, Matsuyama K et al (1995) Disappearance of giant negative T waves in patients with the Japanese form of apical hypertrophy. J Am Coll Cardiol 26:1672–1678
3. Matsubara K, Nakamura T, Kuribayashi T, Azuma A, Nakagawa M (2003) Sustained cavity obliteration and apical aneurysm formation in apical hypertrophic cardiomyopathy. J Am Coll Cardiol 42:288–295
4. Nakamura T, Furukawa K, Matsubara K (1990) Long-term follow-up of electrocardiographic changes in patients with asymmetric apical hypertrophy. J Cardiol 20:635–647
5. Sakamoto T (2001) Apical hypertrophic cardiomyopathy (apical hypertrophy): an overview. J Cardiol 37(Suppl I):161–178
6. Sakamoto T, Tei C, Murayama M, Ichiyasu H, Hada Y, Hayashi T (1976) Giant T wave inversion as a manifestation of asymmetrical apical hypertrophy (AAH) of the left ventricle. Jpn Heart J 17:611–629
7. Webb JG, Sasson Z, Rakowski H, Peter L, Wigle ED (1990) Apical hypertrophic cardiomyopathy: clinical follow-up and diagnosis correlates. J Am Coll Cardiol 15:83–90
8. Yamaguchi H, Ishimura T, Nishiyama S et al (1979) Hypertrophic nonobstructive cardiomyopathy with giant negative T waves (apical hypertrophy): ventriculographic and echocardiographic features in 30 patients. Am J Cardiol 44:401–412

00 00 00 00 00 00 00 00 04 95 24

CASE REPORTS

Coronary Artery Dilatation in LEOPARD Syndrome. A Child Case and Literature Review

Yoko Iwasaki, MD,* Hitoshi Horigome, MD, PhD,* Miho Takahashi-Igari, MD,* Yoshiaki Kato, MD,* M. Abdur Razzaque, PhD,† and Rumiko Matsuoka, MD, PhD†

*Department of Child Health, Graduate School of Comprehensive Human Sciences, University of Tsukuba, Tsukuba; †Division of Pediatric Cardiology, International Research and Educational Institute for Integrated Medical Sciences, Tokyo Women's Medical University, Tokyo, Japan

ABSTRACT

LEOPARD syndrome (LS) is a rare inherited disease with multiple somatic abnormalities. LS and Noonan syndrome (NS) share many features, including cardiovascular disorders, and PTPN11 gene mutation is commonly reported in both syndromes. We report a 10-year-old male patient who was diagnosed as LS based on typical phenotypes including multiple lentigines, electrocardiographic abnormalities, ocular hypertelorism and deafness. Although the most prevalent cardiovascular abnormalities in LS are pulmonary stenosis and hypertrophic cardiomyopathy, diffuse bilateral dilatation of the coronary arteries was found on angiography in addition to apical hypertrophic cardiomyopathy in the present case. The vessels showed slight increases in diameter on angiography conducted at an interval of 6 years. A literature review identified several case reports describing coronary ectasia in patients with NS as well as LS. Considering both syndromes share the mutation of PTPN11 gene, coronary arterial involvement could be related to the gene aberration and should be screened even if the patient shows no symptoms of ischemic heart disease.

Key Words. Coronary Artery Dilatation; LEOPARD Syndrome; *PTPN11* Gene

Introduction

LEOPARD syndrome (LS) is an autosomal dominant inherited disorder characterized by multisystemic abnormalities including multiple Lentigines, Electrocardiographic abnormalities, Ocular hypertelorism, Pulmonary stenosis, Abnormalities of genitalia, Retardation of growth, and Deafness. LS shares many phenotypes with Noonan syndrome (NS), although lentigines and deafness are usually not present in the latter, though protein tyrosine phosphatase, nonreceptor-type 11 (*PTPN11*) gene mutation is commonly observed in both syndromes.[1] Pulmonary stenosis and hypertrophic cardiomyopathy are the most common cardiac abnormalities in patients with NS as well as those with LS.[1] We report a patient with LS and apical hypertrophic cardiomyopathy who also had diffuse bilateral dilatation of coronary arteries.

Case Report

A 10-year-old boy was referred to our hospital for evaluation of the cardiovascular system. The patient had been diagnosed with LS at age 5 based on characteristic features, including multiple lentigines, ocular hypertelorism, growth retardation, and sensorineural hearing loss. Electrocardiography showed left axis deviation and low-voltage T wave in the inferiolateral leads without ST segment deviation. Family history showed no significant inherited phenotype suggestive of LS or cardiovascular disease. Echocardiography on admission showed myocardial hypertrophy of the septum and apical portions. Septal hypertrophy was not prominent with maximum thickness of the interventricular septum of 10 mm. Cardiac catheterization was then conducted. There was no pressure gradient in both the right and left ventricular outflow

© 2009 Copyright the Authors
Journal Compilation © 2009 Wiley Periodicals, Inc.

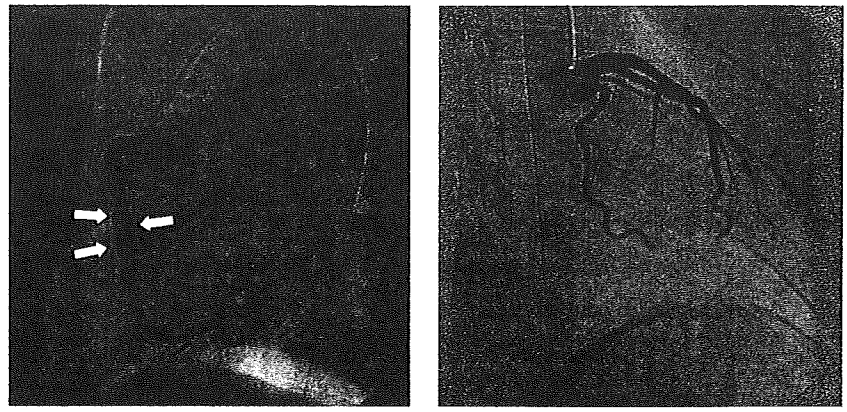

Figure 1. Coronary arteriograms at age 16, showing diffuse bilateral dilatation of coronary arteries without thrombus formation in the lumen. Arrows indicate slightly irregular vessel wall of the right coronary artery.

tracts. Selective coronary angiography revealed diffuse bilateral dilatation of coronary arteries with a maximum diameter of 6.8 mm for the right and 5.7 mm for the left anterior descending branch. There was no coronary arterial fistula or aneurysm formation indicative of Kawasaki disease.

Follow-up coronary arteriography performed at age 16 revealed slight increase in the vessel diameter, with a maximum diameter of 7.9 mm for the right and 7.3 mm for the left anterior descending branch. The vessel wall of the right coronary artery was slightly irregular (Figure 1). Squeezing of the peripheral portion of the right coronary artery was also noted. Left ventriculography showed the characteristic shape of apical hypertrophic cardiomyopathy (Figure 2). However, electrocardiography still showed no ST deviation. *PTPN11* gene sequence analysis using peripheral blood identified a missense mutation in exon 7 (Tyr279Cys).

The patient did not complain of chest pain, arrhythmias or other cardiac symptoms during the follow-up period of 12 years without any medication.

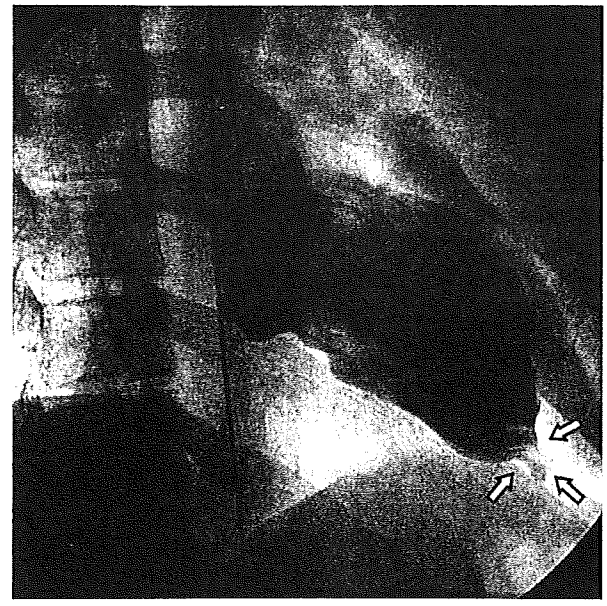

Figure 2. Left ventriculogram at age 16, showing a typical configuration of left ventricular cavity to apical hypertrophic cardiomyopathy (arrows).

Discussion

The present case demonstrated that LS can be complicated by coronary artery dilatation as well as hypertrophic cardiomyopathy and pulmonary stenosis. Aneurysm formation or ectasia of coronary arteries is usually the secondary manifestation of a congenital coronary fistula or, more prevalently, Kawasaki disease; both disorders could be excluded in the present case based on history taking and angiography. A careful search of the 1990–2008 PubMed database identified five reported cases of LS complicated with coronary artery dilatation[2–4] (Table 1). Four of them were recently reported by Limongelli et al.[4] among 26 patients with LS (one of them overlapped with the case of reference[3]). Thus, the estimated incidence of coronary dilatation in LS is 15%. Four out of the five reported cases had *PTPN11* mutation as in the present case. Although the type of *PTPN11* mutation varied among cases, one had the same mutation (Tyr279Cys) and showed LV morphological abnormality similar to our case.[3]

It is intriguing that coronary artery dilatation has also been demonstrated in patients with NS,

Table 1. Noonan Syndrome and LEOPARD Syndrome with Coronary Dilatation

Case	Authors (year)	Reference no.	Age/Gender	LS or NS	Cardiac Manifestation	*PTPN11* Mutation
1	Nomura et al. (2000)	5	10/M	NS	HOCM	ND
2	Ucar et al. (2005)	6	12/F	NS	CAN, PS, ASD, VSD	ND
3	Wong et al. (1990)	7	23/M	NS	CoA, AVA, PDA	ND
4	Loukas et al. (2004)	8	26/F	NS	PS	ND
5	Limongelli et al. (2007)	4	2	LS	AVA, MVA	Thr468Met
6	Limongelli et al. (2007)	4	7	LS	PS, MVA, LVS	Tyr279Cys
7	Pacileo et al. (2006)	3	13/M	LS	HOCM	Exon 13, Arg498Leu
8	Hagspiel et al. (2005)	2	17/M	LS	PS, HOCM	ND
9	Limongelli et al. (2007)	4	39	LS	HOCM	Negative
10	Present case	—	10/M	LS	APH	Exon7 Tyr279 Cys

APH, apical hypertrophic cardiomyopathy; Arg, arginine; ASD, atrial septal defect; AVA, aortic valve abnormalities; CAN, coronary aneurysm; CoA, coarctation of aorta; Cys, cysteine; HOCM, hypertrophic obstructive cardiomyopathy; Leu, leucine; LS, LEOPARD syndrome; LVS, left ventricular shape abnormality; Met, methionine; MVA, mitral valve abnormalities; ND, not described; NS, Noonan syndrome; PDA, patent ductus arterioles; PS, pulmonary stenosis; Thr, threonine; Tyr, tyrosine; VSD, ventricular septal defect.

because *PTPN11* gene mutation has been identified in both syndromes. A careful search of the 1990–2008 PubMed database identified four reported cases of NS complicated with coronary dilatation, [5–8] including a case with giant aneurysm reported by Wong et al.[7] (Table 1). It is known that LS and NS have common cardiovascular manifestations, pulmonary stenosis, and hypertrophic cardiomyopathy, although the most common heart defect is different between the two syndromes. In NS, pulmonary stenosis is the most common and is associated with a codon 308 mutation hot spot.[1] On the other hand, hypertrophic cardiomyopathy is the most common in LS in association with mutation hot spots in exons 7 and 12.[1] Screening for coronary artery abnormalities is important in the management of patients with LS and NS because thrombus formation can develop in dilated coronary arteries. Also, prophylactic administration of anticoagulant and antiplatelet drugs was recommended in previous reports,[5] although ischemic heart disease associated with thrombus formation has not been reported in LS and NS with dilated coronary arteries. Surgical resection or reconstruction should also be considered for large coronary aneurysms to avoid complications such as rupture, thrombosis, and coronary embolization. However, the size criteria of surgical intervention in an asymptomatic patient have not been established, and most of the patients who underwent surgery in the literature had a giant aneurysm, e.g., >50 mm in diameter.[9] Therefore, simple observation or conservative therapy with antiplatelet drugs is justifiable for our patient. Further studies in a large number of patients are needed to determine whether prophylactic anticoagulation therapy and surgery should be considered in LS and NS.

Coronary artery ectasia because of atherosclerosis is rather common in adulthood, and two mechanisms have been proposed.[10] The favorable one is severe and chronic inflammation and the less favorable is vascular overstimulation by exogenous interstitial nitric oxide. The involvement of metalloproteinases and plasma soluble adhesion molecules was also reported as a possible mechanism. However, the abovementioned pathologies have not been reported in LS or NS, and are also unlikely in the present case. As a congenital mechanism of coronary ectasia, jet blood flow produced by bicuspid aortic valve was reported in three neonates.[11] Although the presence of bicuspid aortic valve is common in NS, the present case did not have such a lesion. Further, the dilated site produced by jet flow tends to be confined to the proximal portion of the coronary artery,[11] compared with the present case which showed diffuse dilatation at longer segments.

Although *PTPN11* gene mutation is a possible background of many kinds of congenital heart defects and is possibly involved in coronary dilatation, its role in the pathogenesis remains to be clarified. *PTPN11* gene maps to chromosome 12q22-pter and encodes the human Shp2, the nonreceptor-type protein tyrosine phosphatase, which is a signal-enhancing component of growth factor, cytokine, and extracellular matrix receptor signaling.[12] Shp2 is involved in the signaling cascade of the vascular endothelial growth factor through interaction with the angiopoietin-1 receptor (Tie-2), and exerts mitogenic effects on vascular smooth muscle cells under the nitric oxide-induced pathway.[13] These mechanisms may explain the vascular abnormalities, including coronary dilatation in LS patients. However, *PTPN11* mutations were evident in approximately 60–80% of LS and 30–50% of NS reported in the literature,[1,4,14] and mutations are located in the different domain of the protein. Further, a number of genes of the Ras mitogen-activated protein kinase

pathway are involved in the pathogenesis of LS and NS.[14] It is unclear how the specific mutation Tyr279Cys is causing the different phenotype. It is possible that there might be other genes or single nucleotide polymorphisms associated with coronary dilatation in LS. Further studies are needed to elucidate how the genotype influences the clinical phenotype in LS patients.

Conclusion

LS and NS share multisystemic phenotypes including abnormalities in cardiovascular system as well as *PTPN11* gene mutation. Coronary artery dilatation is an additional important cardiovascular complication in both syndromes, and we recommend screening such patients even if they show no symptoms of ischemic heart disease.

Corresponding Author: Hitoshi Horigome, MD, PhD, Department of Child Health, Graduate School of Comprehensive Human Sciences, University of Tsukuba, Tsukuba, Japan. Tel: (+81) 29-853-3210; Fax: (+81) 29-853-5635; E-mail: hhorigom@md.tsukuba.ac.jp

Conflict of interest: None.

Accepted in final form: October 15, 2008.

References

1 Sarkozy A, Conti E, Seripa D, et al. Correlation between PTPN11 gene mutation and congenital heart defects in Noonan and LEOPARD syndromes. *J Med Genet.* 2003;40:704–708.
2 Hagspiel KD, Candinas RC, Hagspiel HJ, Amann FW. LEOPARD syndrome: cardiac imaging findings. *AJR.* 2005;184:S21–S24.
3 Pacileo G, Calabro P, Limongelli G, et al. Diffuse coronary dilatation in a young patient with LEOPARD syndrome. *Int J Cardiol.* 2006;112:e35–e37.
4 Limongelli G, Pacileo G, Marino B, et al. Prevalence and clinical significance of cardiovascular abnormalities in patients with the LEOPARD syndrome. *Am J Cardiol.* 2007;100:736–741.
5 Nomura Y, Yanagi S, Kono Y, et al. Bilateral coronary artery dilatation in a child with Noonan syndrome. *Jpn Circ J.* 2000;64:481–483.
6 Ucar T, Atalay S, Tekin M, Tutar E. Bilateral coronary artery dilatation and supravalvular pulmonary stenosis in a child with Noonan syndrome. *Pediatr Cardiol.* 2005;26:848–850.
7 Wong CK, Cheng CH, Lau CP, Leung WH. Congenital coronary artery anomalies in Noonan's syndrome. *Am Heart J.* 1990;119:396–400.
8 Loukas M, Dabrowski M, Kantoch M, Ruzytto W, Waltenberger J, Giannikopoulas P. A case report of Noonan's syndrome with pulmonary valve stenosis and coronary aneurysms. *Med Sci Monit.* 2004; 10:CS80–CS83.
9 Mawatari T, Koshino T, Morishita K, Komatsu K, Abe T. Successful surgical treatment of giant coronary artery aneurysm with fistula. *Ann Thorac Surg.* 2000;70:1394–1397.
10 Manginas A, Cokkinos DV. Coronary artery ectasias: imaging, functional assessment and clinical implications. *Eur Heart J.* 2006;27:1026–1031.
11 Chakrabarti S, Thomas E, Wright JGC, Vettukattil JJ. Congenital coronary artery dilatation. *Heart.* 2003;89:595–596.
12 Keilhack H, David FS, McGregor M, Cantley LC, Neel BG. Diverse biochemical properties of Shp2 mutants. Implications for disease phenotypes. *J Biol Chem.* 2005;280:30984–30993.
13 Chang Y, Ceacareanu B, Dixit M, Sreejayan N, Hassid A. Nitric oxide-induced motility in aortic smooth muscle cells: role of protein tyrosine phosphatase SHP-2 and GTP-binding protein Rho. *Cir Res.* 2002;91:390–397.
14 Razzaque MA, Nishizawa T, Komoike Y, et al. Germline gain-of-function mutations in RAF1 cause Noonan syndrome. *Nat Genet.* 2007;39:1013–1017.